Chemical Science

Accepted Manuscript

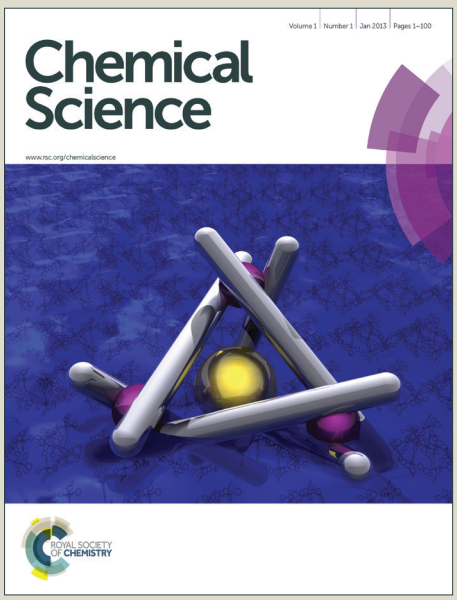

ROYAL SOCIETY OF CHEMISTRY

www.rsc.org/chemicalscience

Journal Name

ARTICLE

Bridging cells of three colors with two bio-orthogonal click reactions

Received 00th January 20xx,
Accepted 00th January 20xx

DOI: 10.1039/x0xx00000x

www.rsc.org/

Yue Yuan,‡[a] Di Li,‡[b] Jia Zhang,[a] Xianmin Chen,[a] Chi Zhang,[c] Zhanling Ding,[a] Lin Wang,[d] Xueqian Zhang,[a] Junhua Yuan,[c] Yinmei Li,[b] Yanbiao Kang,[a] and Gaolin Liang*[a]

Cell-cell interactions play a crucial role in the development and function of multicellular organisms. To study cell-cell interactions in vitro, it is a big challenge for researchers to artificially build up cell junctions to bridge different types of cells for this purpose. Herein, by employing two orthogonal click reactions, we rationally designed four click reagents **Mal-CBT**, **Mal-Cys**, **Mal-Alkyne**, and **Mal-N_3** and successfully applied them for bridging cells of three colors. Orthogonality between these two click reactions was validated in solution and characterized with HPLC and ESI-MS analyses. After modifications of fluorescent protein-expressing prokaryotic *Escherichia coli* (*E. Coli*) cells (or eukaryotic HEK 293T cells) of three colors with respective **Mal-Cys**, **Mal-CBT** and **Mal-Alkyne**, or **Mal-N_3**, the cells were sequentially bridged. The HEK 293T cells showed higher efficiency of cell bridging than that of *E. Coli* cells. At last, using optical tweezers, we quantitatively measured the bridging probability between **Mal-Cys**-modified and **Mal-CBT**-modified HEK 293 cells, as well as the rupture force between two bridged cells. We found that the CBT-Cys click reaction markedly improved the efficiency of cell bridging and the rupture force between two bridged cells was measured to be 153.8 pN at a force-loading rate of 49 pN/s. Our results demonstrate that it is possible to use two (or n) orthogonal click reactions to bridge three (or n + 1) types of cells. Taken the biological importance of cell junctions into consideration, we anticipate our method of bridging three types of cells with two bio-orthogonal click reactions to be a useful tool for biologists to study cell-cell interactions with more convenience and efficiency.

Introduction

Cell-cell interactions between cell surfaces play a crucial role in the development and function of multicellular organisms. Through these interactions, cells are able to communicate with each other in response to their microenvironmental change. But the loss of communication between cells can result in uncontrollable cell growth and cancer.[1-3] Cell interactions can be stabilized through cell junctions. Cell junction (or intercellular bridge) is one type of structure that exists within the tissue of some multicellular organisms (e.g., animals), and is especially abundant in epithelial tissues.[4-6] Normally, cell junctions are consisted of multi-protein complexes.[4] On one hand, cell membranes in the tissues of junctional surfaces are normally so permeable that many cellular ions and molecules may diffuse freely from one cell interior to that of the next.[5] On the other hand, cell junctions build up the paracellular barrier between cells and control the paracellular transport.[7] In consideration of the biological importance of cell interaction, it is a big challenge for people to artificially build up cell junctions to bridge different types of cells and study their behavior. For example, to bridge three types of cells with chemical approach, two bio-orthogonal reactions are needed to fulfill this. Nevertheless, to the best of our knowledge, there has been no report on bridging three types of cells directly with two bio-orthogonal click reactions.

Bio-orthogonal reactions are chemical reactions that the participating functional groups selectively react with each other under biocompatible conditions by neither interacting with nor interfering with the biological system.[8] The use of bio-orthogonal chemistry to probe biomolecules in living systems typically follows a two-step process: first, a small chemical reporter (e.g., an aldehyde, azide, alkyne, or alkene) is site-selectively introduced into the biomolecule(s) of interest via an appropriate biosynthetic or biochemical pathway; then, a biophysical probe carrying the cognate reactive group bio-orthogonally reacts with the reporter in situ to selectively ligate the pre-tagged biomolecule(s) of interest.[9]

[a] CAS Key Laboratory of Soft Matter Chemistry, Department of Chemistry, University of Science and Technology of China, Hefei, Anhui 230026, China.
[b] Hefei National Laboratory for Physical Sciences at the Microscale, Department of Optics and Optical Engineering, University of Science and Technology of China, Hefei, Anhui, 230026, China.
[c] Hefei National Laboratory for Physical Sciences at the Microscale, Department of Physics, University of Science and Technology of China, Hefei, Anhui, 230026, China.
[d] School of Life Sciences, University of Science and Technology of China, Hefei, Anhui 230027, China.
E-mail: gliang@ustc.edu.cn (G. L.).
† Electronic Supplementary Information (ESI) available: Supplementary Schemes. S1-S7; Supplementary Figs. S1-S19; Supplementary Tables S1-S2; Supplementary Videos S1-S3. See DOI: 10.1039/x0xx00000x
‡ These authors contributed equally to this work.

Using bio-orthogonal approaches, people have gained new insights into a wide range of biological processes, such as glycome imaging,[10] protein lipidation and lipid trafficking,[11] and activity-based protein profiling.[12,13] In the early years of this century, Sharpless and co-workers defined click reaction as the one that is highly selective and efficient, wide in scope, easy to perform, uses readily available reagents, and is insensitive to oxygen and water. Work-up and isolation of the product of a click reaction must be simple, without requiring chromatographic purification.[14-16] To date, click reactions have shown their specific advantages in bio-orthogonal probing of biomarkers, cell labeling, and tumor-targeted imaging.[17-22]

Considering the biological importance of cell interactions, we proposed to choose two bio-orthogonal click reactions to bridge three types of cells. Firstly, a thiol-based click condensation reaction between 2-cyanobenzothiazole (CBT) and $_D$-cysteine ($_D$-Cys) developed by Rao and co-workers was chosen for this purpose.[23-25] This click reaction takes place in the luciferin-regenerating pathway of a firefly body with high efficiency and biocompatibility. It has been successfully applied in the preparations of oligomeric nanostructures, molecular imaging (e.g., optical imaging, nuclear imaging, and magnetic resonance imaging), biomolecular detection, and other potentialities.[26-28] At pH 7.4 in water, this click reaction occurs spontaneously between the CBT-Cys pair to yield a thiazole ring which covalently bridges two types of cells. Then, the Cu(I)-catalyzed azide-alkyne click cycloaddition was chosen to bio-orthogonally bridge the third type of cells. Because the azide-alkyne click cycloaddition has been extensively exploited and widely used in bioconjugate applications.[29] After cell bridging, the bridging probability between two cells and the rupture force of bridged cells were quantitatively measured by optical tweezers. Optical tweezzers have been widely used in single-molecule biology[30] and cytobiology[31,32] due to their advantage in non-contact manipulation and the ability of quantitative measurement of piconewton force.

Results and discussion

Despite the fact that the individual CBT-Cys condensation or azide-alkyne cycloaddition has shown to be compatible with biological systems, their site-specific double incorporations have not yet been demonstrated. Therefore, we first validated the orthogonality between these two click reactions, and then used these two bio-orthogonal click reactions for bridging three types of cells. As shown in Fig. 1a, compounds **Mal-CBT**, **Mal-Cys**, **Mal-Alkyne**, and **Mal-N_3** containing the bio-orthogonal functional groups for click reactions and maleimide groups for conjugating the –SH groups on cell walls (or membranes) were designed and synthesized. The synthetic routes and characterizations of these four compounds were shown in Electronic Supplementary Information (ESI†, Schemes S1-S4† and Figs. S1-S7†). Since compound **Mal-N_3** is unstable, we used **Mal-NHS** and **N_3-NH_2** to freshly prepare **Mal-N_3** for the cell-bridging experiment. Feasibility of this reaction was testified and shown in the ESI† (Scheme S4† and Figs. S6-S7†). Fig. 1b schematically shows the procedure of cell-bridging. In detail, **Mal-Cys**-modified cell **A** was bridged with cell **B** that was modified with both **Mal-CBT** and **Mal-Alkyne** via CBT-Cys condensation under reduction condition. Then the **Mal-Alkyne** modified cell **B** on the **A-B** cell pair was bridged with **Mal-N_3**-modified cell **C** under the catalysis of Cu^+ to form the **A-B-C** cell complex.

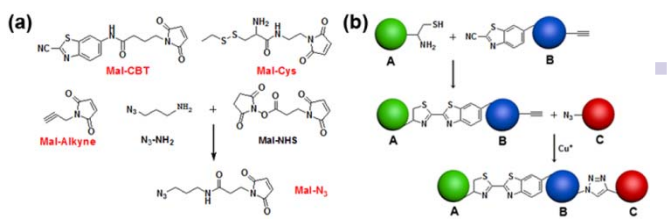

Fig. 1 (a) Chemical structures of compounds **Mal-CBT**, **Mal-Cys**, **Mal-Alkyne**, and **Mal-N_3** containing the bio-orthogonal functional groups for click reactions. (b) Schematic illustration of bridging three types of cells with two bio-orthogonal click reactions.

Validation of orthogonality between CBT-Cys condensation and azide-alkyne cycloaddition. When compound **Mal-Cys** was treated with reducing agents (e.g., tris(2-carboxyethyl)-phosphine, TCEP) to expose the cysteine motif for click condensation, the resulting –SH group would also react with the itself maleimide motif. Therefore, to validate the orthogonality between the two click reactions, we firstly used mercaptoethanol (MCH) to react with the maleimide groups of compounds **Mal-CBT**, **Mal-Cys**, and **Mal-Alkyne** to prepare respective compounds **1**, **2**, and **3**, as shown in Fig. 2a. The synthetic routes and characterizations of **1**, **2**, and **3** were shown in the ESI† (Schemes S5-S7† and Figs. S8-S10†). 100 μM **1**, 100 μM **2**, and 400 μM TCEP were together dissolved in 500 μL phosphate buffer (pH 7.4, 0.1 M), then the mixture solution was shaken for 1 hour at room temperature (RT) before being injected into a high-performance liquid chromatography (HPLC) system for analysis. As shown by the green HPLC trace in Fig. 2b, only the title product **4** of the click reaction between **1** and **2** was cleanly obtained, which was testified by the electron-spray ionization mass (ESI-MS) result in Fig. S11 (ESI†). Similarly, 100 μM **3**, 100 μM **N_3-NH_2**, 1 mM $CuSO_4$, and 7 mM NaVc were dissolved in 500 μL phosphate buffer (pH 7.4, 0.1 M) and then the mixture solution was shaken for 1 hour at RT. HPLC analysis indicated that only the title product **5** of click reaction between **3** and **N_3-NH_2** was cleanly obtained (blue HPLC trace in Fig. 2b), proven by the ESI-MS result in Fig. S12 (ESI†). Then we investigated the orthogonality of these two click reactions. 50 μM **1**, 50 μM **2**, 50 μM **3**, and 200 μM TCEP were dissolved in 500 μL phosphate buffer (pH 7.4, 0.1 M) and shaken for 30 min at RT. Then 100 μM **N_3-NH_2**, 0.5 mM CuSO4, and 3.5 mM NaVc were added to above mixture and shaken for another 1 hour at RT. As shown by the magenta HPLC trace in Fig. 2b, except the title compounds **4** and **5**, there was no new compound appeared on the trace, suggesting that the CBT-Cys click condensation and azide-alkyne click cycloaddition are orthogonal. To further confirm the completion of the reactions, we studied the kinetics of these CBT-Cys click condensation and azide-alkyne click cycloaddition reactions and their second-order rate constants were measured to be 27.8 $M^{-1}s^{-1}$ and 19.7 $M^{-1}s^{-1}$ at this condition, respectively (Figs. S13-S14†).

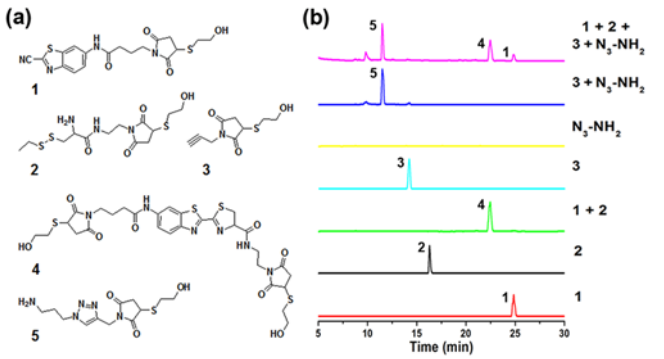

Fig. 2 (a) Chemical structures of compounds **1**-**5** in this work. (b) HPLC traces of **1** (red); **2** (black); 100 μM **1**, 100 μM **2**, and 400 μM TCEP dissolved in 500 μL phosphate buffer (pH 7.4, 0.1 M) and shaken for 1 hour at RT (green); **3** (cyan); **N_3-NH_2** (yellow); 100 μM **3**, 100 μM **N_3-NH_2**, 1 mM CuSO4, and 7 mM NaVc dissolved in 500 μL phosphate buffer (pH 7.4, 0.1 M) and shaken for 1 hour at RT (blue); 50 μM **1**, 50 μM **2**, 50 μM **3**, and 200 μM TCEP dissolved in 500 μL phosphate buffer (pH 7.4, 0.1 M) and shaken for 30 min at RT, then 100 μM **N_3-NH_2**, 0.5 mM CuSO4, and 3.5 mM NaVc were added to above mixture and shaken for another 1 hour at RT (magenta).

Bridging prokaryotic cells in three colors. After validating the orthogonality between these two click reactions, we started to use them to bridge prokaryotic cells in three colors. Three colors of *Escherichia coli* (*E. coli*) cells that respectively express green (eGFP), yellow (eYFP), or red (mCherry, RFP) fluorescent proteins were used for the following experiments. Before being conjugated to click reagents, the cells were incubated with 1 mM TCEP at 37 °C for 30 min to expose the -SH groups on their surface proteins, washed with phosphate-buffered saline (PBS, pH 7.4, 10 mM) for three times by centrifugation at 8,000 rpm and 4 °C. Then the GFP^+ cells with 0.5 mM **Mal-Cys**, YFP^+ cells with 1 mM **Mal-CBT** and 1 mM **Mal-Alkyne** were respectively incubated at 37 °C for 1 h, washed with PBS for three times by centrifugation at 8,000 rpm and 4 °C. Then the **Mal-Cys**-treated GFP^+ cells (15.4% of **Mal-Cys** was loaded to the GFP^+ cells, calculated by HPLC analysis), together with **Mal-CBT** and **Mal-Alkyne**-treated YFP^+ cells were shaken with 0.5 mM TCEP in PBS at 37 °C for 2 h. The CBT-Cys click reaction efficiency at this condition in the presence of the cells was calculated to be 76.5% by HPLC analysis. As shown in Fig. 3a, half of the GFP^+ cells were bridged with YFP^+ cells (8 of total 16 cells in the view field). Note here that the blue fluorescence emission from YFP^+ cells was resulted from the fluorescent compound **Mal-CBT**. Interestingly, in the absence of TCEP, the click reagent-treated GFP^+ and YFP^+ cells were not bridged but randomly scattered in the microscopic field, as shown Fig. 3b. This echoes that TCEP is needed to cleave the disulfide bond of **Mal-Cys** to initiate the click condensation. After 10 mM **N_3-NH_2** was shaken with 10 mM **Mal-NHS** in PBS at RT for 1 h, the obtained **Mal-N_3** (diluted to 1 mM) was incubated with RFP^+ cells for at 37 °C for 1 h. Then the **Mal-N_3**-treated RFP^+ cells were shaken with above bridged GFP^+ cells and YFP^+ cells together in PBS containing 1 mM $CuSO_4$, and 7 mM NaVc at 37 °C for 2 h. As shown in Fig. 3c, some of the RFP^+ cells were bridged with single YFP^+ cells or with YFP^+ cells on the YFP^+-GFP^+ cell pair, suggesting that the azide-alkyne click cycloaddition really happened. Microscopic image of the bridged prokaryotic cells at lower magnification with more cells was shown in Fig. S15 (ESI†). Stability study indicated that the conjunctions among the bridged prokaryotic cells were stable in PBS for 48 h at RT. Interestingly, we could not find the RFP^+ cells directly bridge with GFP^+ cells, echoing that the CBT-Cys click condensation and azide-alkyne click cycloaddition are orthogonal. If the RFP^+ cells were not modified with **Mal-N_3**, mixing the cells with above control YFP^+ cells and GFP^+ cells in Fig. 3b did not result in any bridging among the cells, as shown in Fig. 3d.

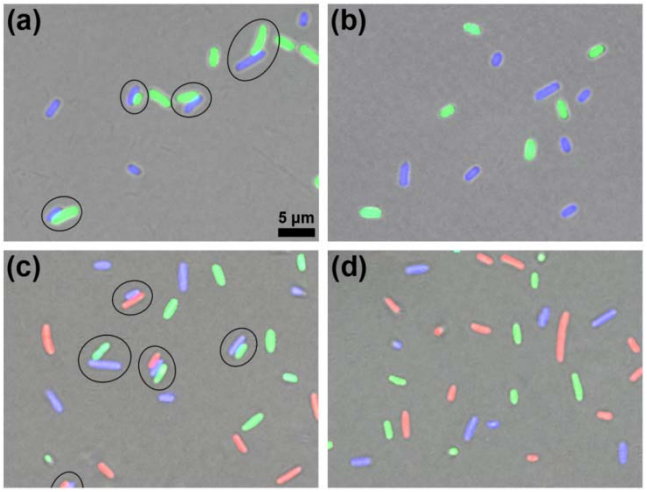

Fig. 3 Microscopic fluorescence images of **Mal-Cys**-treated GFP^+ *E. coli* cells, together with **Mal-CBT** and **Mal-Alkyne**-treated YFP^+ *E. coli* cells after being shaken in the presence (a) or absence (b) of 0.5 mM TCEP in PBS at 37 °C for 2 h. (c) The **Mal-N_3**-treated RFP^+ *E. coli* cells after being shaken with above bridged GFP^+-YFP^+ cells in PBS containing 1 mM $CuSO_4$ and 7 mM NaVc at 37 °C for 2 h. (d) Untreated RFP^+ *E. coli* cells after being shaken with above control GFP^+ cells and YFP^+ cells in Fig. 3b in PBS containing 1 mM $CuSO_4$, and 7 mM NaVc at 37 °C for 2 h.

Bridging eukaryotic cells of three colors. Since the content of proteins in the cytoderm of prokaryotic cells is usually much lower than that in the outer membrane of eukaryotic cells, we applied these two orthogonal click reactions to bridge eukaryotic cells with higher efficiency. HEK 293T cells that respectively transfected with green, blue, or red (DsRed) fluorescent proteins were fixed with 4% paraformaldehyde and used for the following experiments. Before being conjugated with click reagents, HEK 293T cells were incubated with 100 μM TCEP at 37 °C for 30 min, then washed with PBS for three times by centrifugation at 3,000 rpm and 4 °C. After the incubation of GFP^+ cells with 100 μM **Mal-Cys**, BFP^+ cells with both 200 μM **Mal-CBT** and 200 μM **Mal-Alkyne** at 37 °C for 1 h, the cells were washed with PBS for three times by centrifugation at 3,000 rpm and 4 °C (22.6% of **Mal-Cys** was loaded to the GFP^+ cells, calculated by HPLC analysis). Then the GFP^+ cells and BFP^+ cells were shaken together in PBS in the presence of 100 μM TCEP at 37 °C for 1.5 h. The CBT-Cys click reaction efficiency at this condition in the presence of the cells was calculated to be 73.0% by HPLC analysis. As shown in Fig. 4a, most of the GFP^+ cells were bridged with BFP^+ cells (10 of total 11 cells in the field). In the absence of TCEP, the click reagent-treated GFP^+ and BFP^+ cells were not bridged but randomly scattered in the microscopic field, as shown Fig. 4b. Freshly prepared **Mal-N_3** at 200 μM was incubated with RFP^+ cells at 37 °C for 1 h. Then the RFP^+ cells were shaken with above bridged GFP^+ cells and BFP^+ cells in PBS in the presence of 100 μM $CuSO_4$, and 700 μM NaVc at 37 °C for 1.5 h. As shown in Fig. 4c, most of the RFP^+ cells were bridged with either single BFP^+ cells or the BFP^+ cells

on the BFP$^+$-GFP$^+$ cell pair, suggesting that the azide-alkyne click cycloaddition really happened. Microscopic image of the bridged eukaryotic cells at higher density with more cells was shown in Fig. S16 (ESI†). Stability study indicated that the conjunctions among the bridged eukaryotic cells were stable in PBS for 48 h at RT. Similarly, we could not find the RFP$^+$ cells directly bridge with GFP$^+$ cells, additionally echoing that the CBT-Cys click condensation and azide-alkyne click cycloaddition are orthogonal. Without **Mal-N$_3$** modification, RFP$^+$ cells incubated with above control BFP$^+$ cells and GFP$^+$ cells in Fig. 4b did not result in any bridging among the cells in three colors, as shown in Fig. 4d. Interestingly, when the **Mal-CBT**-modified BFP$^+$-HEK 293T cells was replaced with **Mal-CBT**-modified HepG 2 cells, we found that three colors of two different cell lines (HEK 293T cells in green and red, HepG2 in blue) also could be bridged together (Fig. S17†).

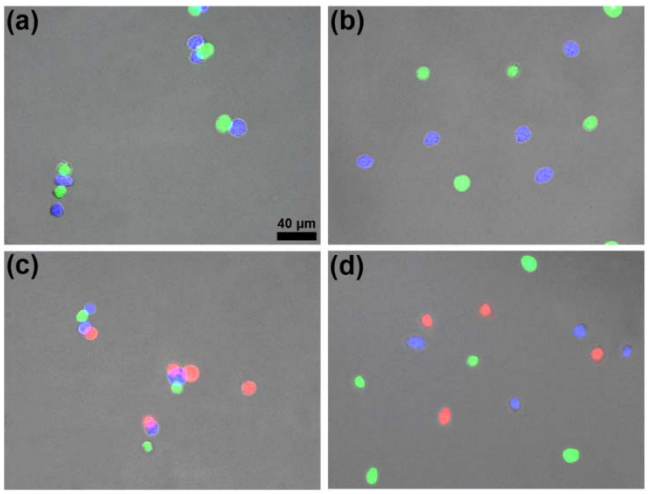

Fig. 4 Microscopic fluorescence images of the **Mal-Cys**-treated GFP$^+$ HEK 293T cells and **Mal-CBT** and **Mal-Alkyne**-treated BFP$^+$ HEK 293T cells after being shaken together in PBS in the presence (a) or absence (b) of 100 μM TCEP at 37 °C for 1.5 h. (c) The **Mal-N$_3$**-treated RFP$^+$ HEK 293T cells after being shaken with above bridged GFP$^+$-BFP$^+$ cells in PBS in the presence of 100 μM $CuSO_4$, and 700 μM NaVc at 37 °C for 1.5 h. (d) Untreated RFP$^+$ HEK 293T cells after being shaken with above control GFP$^+$ cells and BFP$^+$ cells in Fig. 4b in PBS in the presence of 100 μM $CuSO_4$, and 700 μM NaVc at 37 °C for 1.5 h.

Distribution of rupture force of bridged eukaryotic cells. We used optical tweezers to measure the rupture force between **Mal-Cys**-treated GFP$^+$ HEK 293T cells and **Mal-CBT**-treated BFP$^+$ HEK 293T cells in the presence (experimental group) or absence (control group) of 100 μM TCEP. In experiment, the GFP$^+$ cells were distinguished from the BFP$^+$ cells under a fluorescence microscope at first. Then, one GFP$^+$ cell was trapped by optical tweezers and manipulated to contact a BFP$^+$ cell, which adhered to coverslip, for 20 secs. After that, the coverslip started to move at a velocity (v) of 1.4 μm/sec, but the movement of trapped GFP$^+$ cell along with the fixed BFP$^+$ cell would be hindered by an increasing trapping force F, which is induced by an increasing displacement of GFP$^+$ cell departing from the trap center (Δx). From then on, there may be three situations. One situation was that there was no junction between two cells and the two cells were separated immediately, as shown in Fig. S18 and Video S1 (ESI†). For control group, 80.9% of all contact-separation events fell into this situation, while 33.9% of experimental events did, as shown in Table S2 (ESI†). The great

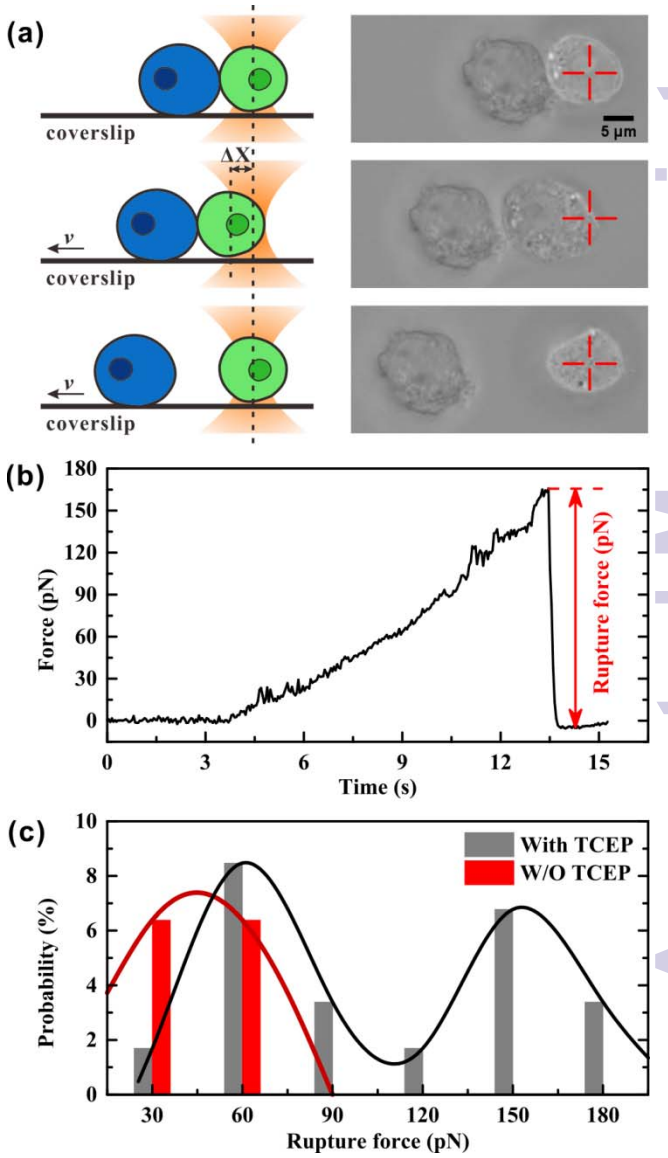

Fig. 5 (a) Sketch (left) and microscopic images (right) for measuring the rupture force between **Mal-Cys**-treated GFP$^+$ HEK 293T cells and **Mal-CBT**-treated BFP$^+$ HEK 293T cells with optical tweezers. (b) Typical force-time curve of the trapped cell. When the trapping force reaches the rupture force (herein 165.7 pN), the bridged GFP$^+$-BFP$^+$ cells are segregated, and the force drops to zero rapidly. The highest trapping force can be regarded as the rupture force of bridged GFP$^+$-BFP$^+$ cells. (c) Histogram of rupture forces of bridged GFP$^+$-BFP$^+$ cells. The gray bars and black solid line are the measurement results of rupture force of bridged GFP$^+$-BFP$^+$ cells in the presence of 100 μM TCEP. The red bars and crimson solid line are the measurement results of **Mal-Cys**-treated GFP$^+$ HEK 293T cells and **Mal-CBT**-treated BFP$^+$ HEK 293T cells in the absence of TCEP.

difference of this probability between these two groups of cells demonstrated that the click condensation reaction can bridge eukaryotic cells with very high efficiency. The second situation was that there were junctions between the GFP$^+$ and BFP$^+$ cells but the bridged cells could be separated by the trapping force, as shown in Fig. 5a and Video S2 (ESI†). In this case, the optical tweezer-trapped GFP$^+$ cell moved along with the BFP$^+$ cell at the beginning and at a force-loading rate of 49 pN/s. Once the trapping force was higher than the rupture force of bridged GFP$^+$-BFP$^+$ cells, two cells would be separated and the trapping force would drop to zero rapidly, as shown in Fig. 5b. The highest trapping force during stretching could

be regarded as the rupture force. Fig. 5c illustrated the histogram of the rupture forces. There was only one histogram peak at a value of 45.0 pN for control group. However, for experimental group, besides a histogram peak at a value of 60.6 pN closing to that of control group, there was an extra histogram peak at 153.8 pN which was of the same order of magnitude of the force of silicon-carbon bond reported.[33] Therefore, this extra peak in experimental group should be ascribed to the covalent bond formed in CBT-Cys click reaction between the bridged GFP^+-BFP^+ cells. The third situation was that the bridged GFP^+-BFP^+ cells could not be ruptured by trapping force before the GFP^+ cell escaped from the optical trap, as shown in Fig. S19 and Video S3 (ESI†). In this case, the rupture force exceeded the measuring range of our optical tweezers (about 200 pN). For control group, 6.4% of all contact-separation events fell into this situation. This might be ascribed to the non-specific interactions between GFP^+ and BFP^+ cells. For experimental group, the probability of this case was 40.7%, which was much higher than that of control group, as shown in Table S2 (ESI†). We presume that this might be cause by multiple click reactions in one pair of bridged GFP^+-BFP^+ cells and the non-specific interactions, and the former should be dominant. In this work, 71 contact-separation events included in above three situations were measured by optical tweezers for experimental group, and 63 contact-separation events were measured for control group.

Conclusions

In summary, employing two click reactions (click condensation of CBT-Cys and click cycloaddition of azide-alkyne), we rationally designed four click reagents **Mal-CBT**, **Mal-Cys**, **Mal-Alkyne**, and **Mal-N_3** for bridging cells of three colors. Orthogonality between these two click reactions was validated in solution, characterized with HPLC and ESI-MS analyses. After modifications of different colors of fluorescent protein prokaryotic cells of *E. Coli* with respective **Mal-Cys**, **Mal-CBT** and **Mal-Alkyne**, or **Mal-N_3,** the cells were sequentially bridged. We also modified GFP^+-, BFP^+-, or RFP^+-eukaryotic cells of HEK 293T cells with these four click reagents and sequentially bridged them with higher efficiency. Using optical tweezers, we quantitatively measured the bridging efficiency of eukaryotic cells and the rupture force of bridged cells to be 153.8 pN. In consideration of the biological importance of cell junctions, we envisioned that our method of bridging three (or n + 1) types of cells with two (or n) bio-orthogonal click reactions might aid biologists to study cell-cell interactions *in vitro* with more convenience and efficiency.

Experimental

Materials and methods

All the starting materials were obtained from Sigma-Aldrich, Adamas, or Sangon Biotech. Commercially available reagents were used without further purification, unless noted otherwise. All chemicals were reagent grade or better. pBAD-GFP expresses eGFP from an arabinose-inducible promotor on a pBAD vector. pVS132 expresses eYFP from a IPTG-inducible promotor on a pTrc99a vector. pAmCherry1 was expressed from the plasmid pAmCherry1-N1. The fluorescent plasmids transfected to HEK 293T cells were generously provided by Prof. Bing Hu and Prof. Guoqiang Bi of University of Science and Technology of China (USTC). PBS used for cell experiment was prepared with PBS pills from Sangon Biotech. Milli-Q water (18.2 MΩcm) was used throughout the experiment. The spectra of electrospray ionization-mass spectrometry (ESI-MS) were recorded on a LTQ Orbitrap mass spectrometer (Thermo Fisher). ^{1}HNMR spectra were obtained on 400 MHz Bruker AV 400 or 300 MHz Bruker AV 300. High resolution ESI/MS spectra were obtained on a GCT premier mass spectrometer (Waters). HPLC analyses were performed on an Agilent 1200 HPLC system equipped with a G1322A pump and in-line diode array UV detector using an Agilent Zorbax 300SB-C18 RP column with CH_3CN (0.1% of trifluoroacetic acid (TFA)) and water (0.1% of TFA) as the eluent. Fluorescence microscopic images were taken under a fluorescence microscope OLMPUS IX71.

Synthetic procedures

Preparation of Mal-CBT: 2-cyano-6-aminobenzothiazole (CBT) was synthesized following the literature method (White, E. H., Worther, H., Seliger, H. H., McElroy, W. D. Amino analogs of firefly luciferin and biological activity thereof. J. Am. Chem. Soc. 1966, 88, 2015-2019).

The mixture of 4-Maleimidobutyric acid (18.1 mg, 0.1 mmol), HBTU (41.7 mg, 0.1 mmol), HOBT (13.5 mg, 0.1 mmol) in DMF (2 mL) was stirred for 30 min in presence of DIPEA (11.1 mg, 0.1 mmol), then CBT (26.3 mg, 0.15 mmol) that dissolved in 1 mL of DMF was added into the mixture dropwise. After overnight stirring, compound **Mal-CBT** (10.5 mg, yield: 31%) was obtained after HPLC purification. ^{1}HNMR of compound **Mal-CBT** (d_3-CD_3CN, 300 MHz, Fig. S1†): 8.69 (d, J = 2.00 Hz, 1 H), 8.11 (d, J = 9.01 Hz, 1 H), 7.63 (dd, J_1 = 2.05 Hz, J_2 = 9.01 Hz, 1 H), 6.75 (s, 2 H), 3.54 (t, J = 6.88 Hz, 2 H), 2.39 (t, J = 7.60 Hz, 2 H), 1.92 (m, 2 H). MS: calculated for $C_{16}H_{12}N_4O_3S$ [$(M+H)^+$]: 341.07; obsvd. ESI-MS: m/z 341.02 (Fig. S2†).

Preparation of Mal-Cys: The mixture of N-(2-Aminoethyl)maleimide trifluoroacetate salt (25.4 mg, 0.1 mmol), HBTU (41.7 mg, 0.1 mmol), HOBT (13.5 mg, 0.1 mmol) in DMF (2 mL) was stirred for 30 min in presence of DIPEA (11.1 mg, 0.1 mmol), then Boc-Cys(SEt)-OH (28.1 mg, 0.1 mmol) that dissolved in 1 mL of DMF was added into the mixture dropwise. After overnight stirring, compound Mal-Cys(Boc) (31 mg, yield: 77%) was obtained after HPLC purification. Deprotection of Mal-Cys(Boc) with 95% TFA for 3 h yielded compound **Mal-Cys** after HPLC preparation (18 mg, yield: 77 %). ^{1}HNMR of compound **Mal-Cys** (d_4-CD_3OD, 400 MHz, Fig. S3†): 6.84 (s, 2 H), 4.06 (dd, J_1 = 4.62 Hz, J_2 = 9.24 Hz, 1 H), 3.66 (m, 2 H), 3.31 (m, 2 H), 3.21 (dd, J_1 = 4.59 Hz, J_2 = 14.62 Hz, 1 H), 2.92 (dd, J_1 = 9.18 Hz, J_2 = 14.59 Hz, 1 H), 2.79 (m, 2 H), 1.35 (t, J = 7.29 Hz, 3 H). MS: calculated for $C_{13}H_{22}N_3O_3S_2$ [$(M+H)^+$]: 304.07896; obsvd. HR-GCT/MS: m/z 304.07874 (Fig. S4†).

Preparation of Mal-Alkyne: Refluxing of 3-(prop-2-yn-1-ylcarbamoyl)acrylic acid (160 mg) with xylene (dried with 4Å molecular sieve) for 8 h yielded **Mal-Alkyne** (76 mg, yield: 54%). ^{1}HNMR of compound **Mal-Alkyne** (d_1-$CDCl_3$, 400 MHz, Fig. S5†): 6.71 (s, 2 H), 4.22 (d, J = 2.54 Hz, 2 H), 2.15 (t, J = 2.52 Hz, 1 H).

Preparation of Mal-N_3: The mixture of 3-azido-propylamine (**N_3-NH_2**, 20 mM), N-Succinimidyl 3-maleimidopropionate (**Mal-NHS**, 20 mM) was dissolved in 500 μL phosphate buffer (pH 7.4, 0.1 M). Then compound **Mal-N_3** was obtained after shaking for 1 h at room temperature as the HPLC trace shown (Fig. S6†). MS of compound **Mal-N_3**: calculated for $C_{10}H_{13}N_5O_3$ [$(M+H)^+$]: 252.11; obsvd. ESI-MS: m/z 252.02 (Fig. S7†).

Preparation of 1: The mixture of **Mal-CBT** (100 μL, 100 mM) and mercaptoethanol (MCH, 1 μL) was added into 1 mL phosphate buffer (pH 6.0, 0.2 M), then the mixture was shaken at RT for 5 min. Compound **1** was obtained after HPLC purification. MS of compound **1**: calculated for $C_{18}H_{18}N_4O_4S_2$ [$(M+H)^+$]: 419.08; obsvd. ESI-MS: m/z 419.00 (Fig. S8†).

Preparation of 2: The mixture of **Mal-Cys** (100 μL, 100 mM) and MCH (1 μL) was added into 1 mL phosphate buffer (pH 7.0, 0.2 M), then the mixture was shaken for 10 min at RT. Compound **2** was obtained after HPLC purification. MS of compound **2**: calculated for $C_{13}H_{23}N_3O_4S_3$ [$(M+H)^+$]: 382.09; obsvd. ESI-MS: m/z 382.08 (Fig. S9†).

Preparation of 3: The mixture of **Mal-Alkyne** (100 μL, 100 mM) and mercaptoethanol (MCH, 1 μL) was added into 1 mL phosphate buffer (pH 7.0, 0.2 M), then the mixture was shaken for 30 min at RT. Compound **3** was obtained after HPLC purification. MS of compound **3**: calculated for $C_9H_{11}NO_3S$ [$(M+H)^+$]: 214.05; obsvd. ESI-MS: m/z 214.00 (Fig. S10†).

Optical tweezers measurements

Optical tweezers: The optical tweezers system was as described previously.[31-32] Optical tweezers were built on an inverted fluorescence microscope (Olympus IX71, Japan) using a fiber laser (AFL-1064-40-R-CL, Amonics Limited, Hong Kong) with a wavelength of 1064 nm and a nominal output power of 10 W (Watt). The laser beam was expanded to a diameter of 7 mm to overfill the back-aperture of a water-immersion objective with a high NA of 1.2 (UPLSAPO, 60×, Olympus, Japan). The tightly focused beam can trap dielectric beads or cells steadily in a chamber. When the chamber was moved by a piezoelectric stage (P-545.3R7, PI, Germany), the trapped bead or cell was fixed at an initial location in our field of view. A Charge Coupled Device (CCD) camera (Photometrics CoolSNAP HQ2, America) was used to monitor our manipulations.

Preparation of chambers: Flow chambers were prepared by gluing coverslips to glass slides with holed parafilm. As mentioned above, the **Mal-Cys**-treated GFP^+ HEK 293T cells were incubated with 100 μM TCEP (or without for control group) at 37 °C for 30 min to expose the –SH groups on their surfaces. For the adhesion of the **Mal-CBT**-treated BFP^+ HEK 293T cells to coverslip, chambers were pre-absorbed with poly-$_L$-lysine solution (0.01%, Sigma) for 10 min at RT (25 °C-26 °C). Then chambers were washed with PBS of 10-fold chamber volume, and were incubated with BFP^+ cells for 20 min. After removing of the unbound BFP^+ cells, the GFP^+ cells with blocking reagent at low concentration (0.06% casein, Sigma) were introduced into the chamber. The blocking reagent could prevent the adhesion of GFP^+ cells to coverslips and lessen the non-specificity interactions between GFP^+ cells and BFP^+ cells, but not interfere with the click reactions between GFP^+ cells and BFP^+ cells.

Force measurements: In our experiment, the trapping force meets a linear relationship of $F = -\kappa\Delta x$, where κ is the stiffness of optical trap, Δx is the maximum displacement of cell departing from the trap center. To calibrate the stiffness, the viscosity of assay buffer was calibrated at first. It was calibrated by tracking the free movement of a trapped bead (Thermo scientific, #4205A, 4.993 ± 0.040 μm) after shutting optical trap.[34] In this work, it was calculated to be 1.042×10^{-3} N·s/m^2 under laser power of 1.78 W (laser power in experiment) at objective entrance aperture. Then the stiffness of every GFP^+ cell was calibrated with drag force method at a depth of 20 μm from coverslip.[35] For an optical trap consisted of the water-immersion objective, the stiffness will vary slightly at different depths.[36] Thus, the stiffness can be regarded as a constant at varying depths. To measure the displacement Δx, we used CCD camera to record all movements of GPF^+ and BFP^+ cells. The positions of GFP^+ cells were tracked in image sequences with an image analysis technique of erosion and dilation.[37] Then the force-time curve and rupture force of every bridged GFP^+-BFP^+ cells were measured and calculated.

Acknowledgements

This work was supported by Collaborative Innovation Center of Suzhou Nano Science and Technology, the Major program of Development Foundation of Hefei Center for Physical Science and Technology, the National Natural Science Foundation of China (Grants 21175122, 11374292, and 21375121), and Anhui Provincial Natural Science Foundation (Grant 1508085JGD06).

Notes and references

1 U. Rutishauser, A. Acheson, A. Hall, D. Mann and J. Sunshine, *Science*, 1988, **240**, 53-57.
2 T. G. Wolfsberg, P. Primakoff, D. G. Myles and J. M. White, *J. Cell Biol.*, 1995, **131**, 275-278.
3 G. A. Zimmerman, S. M. Prescott and T. M. McIntyre, *Immunol. Today*, 1992, **13**, 93-100.
4 V. Kumar, R. S. Cotran, S. L. Robbins, *Robbins Basic Pathology* 2003, Saunders.
5 W. R. Loewenstein, Y. Kanno, *Nature,* 1966, **209**, 1248-1249.
6 J. Wiener, D. Spiro, W. R. Loewenstein, *J. Cell Biol.,* 1964, **22,** 587-598.
7 C. M. Van Itallie, J. M. Anderson, *Annu. Rev. Physiol.,* 2006, **68**, 403-429.
8 E. M. Sletten, C. R. Bertozzi, *Acc. Chem. Res.,* 2011, **44**, 666-676.
9 W. Song, Y. Wang, J. Qu, M. M. Madden, Q. Lin, *Angew. Chem. Int. Ed.,* 2008, **47**, 2832-2835.
10 S. T. Laughlin, C. R. Bertozzi, *Proc. Natl. Acad. Sci. U. S. A.,* 2009, **106**, 12-17.
11 H. C. Hang, J. P. Wilson, G. Charron, *Acc. Chem. Res.,* 2011, **44**, 699-708.
12 B. F. Cravatt, A. T. Wright, J. W. Kozarich, *Annu. Rev. Biochem.,* 2008, **77**, 383-414.
13 D. Ye, A. J. Shuhendler, L. Cui, L. Tong, S. S. Tee, G. Tikhomirov, D. W. Felsher, J. Rao, *Nat. Chem.,* 2014, **6**, 519-526.
14 H. C. Kolb, M. G. Finn, K. B. Sharpless, *Angew. Chem. Int. Ed.,* 2001, **40**, 2004-2021.
15 H. C. Kolb, K. B. Sharpless, *Drug Discov. Today,* 2003, **8**, 1128-1137.
16 Y. Yuan, G. L. Liang, *Org. Biomol. Chem.,* 2014, **12**, 865-871.
17 M. D. Best, *Biochemistry,* 2009, **48**, 6571-6584.
18 A. E. Speers, G. C. Adam, B. F. Cravatt, *J. Am. Chem. Soc.,* 2003, **125**, 4686-4687.

19 J. M. Baskin, J. A. Prescher, S. T. Laughlin, N. J. Agard, P. V. Chang, I. A. Miller, A. Lo, J. A. Codelli, C. R. Bertozzi, *Proc. Natl. Acad. Sci. U. S. A.,* 2007, **104**, 16793-16797.
20 E. Saxon, C. R. Bertozzi, *Science,* 2000, **287**, 2007-2010.
21 M. Mammen, S. K. Choi, G. M. Whitesides, *Angew. Chem. Int. Ed.,* 1998, **37**, 2755-2794.
22 Y. Xianyu, Z. Wang and X. Jiang, *ACS Nano*, 2014, **8**, 12741-12747.
23 G. Liang, H. Ren, J. Rao, *Nat. Chem.,* 2010, **2**, 54-60.
24 G. Liang, J. Ronald, Y. Chen, D. Ye, P. Pandit, M. L. Ma, B. Rutt, J. Rao, *Angew. Chem. Int. Ed.,* 2011, **50**, 6283-6286.
25 D. Ye, A. J. Shuhendler, P. Pandit, K. D. Brewer, S. S. Tee, L. Cui, G. Tikhomirov, B. Rutt and J. Rao, *Chem. Sci.*, 2014, **5**, 3845-3852.
26 Y. Yuan, H. Sun, S. Ge, M. Wang, H. Zhao, L. Wang, L. An, J. Zhang, H. Zhang, B. Hu, J. Wang, G. Liang, *ACS Nano,* 2015, **9**, 761-768.
27 S. Liu, A. Tang, M. Xie, Y. Zhao, J. Jiang, G. Liang, *Angew. Chem. Int. Ed.,* 2015, **54**, 3639-3642.
28 Y. Yuan, J. Zhang, L. An, Q. Cao, Y. Deng, G. Liang, *Biomaterials,* 2014, **35**, 7881-7886.
29 Q. Wang, T. R. Chan, R. Hilgraf, V. V. Fokin, K. B. Sharpless, M. G. Finn, *J. Am. Chem. Soc.,* 2003, **125**, 3192-3193.
30 J. R. Moffitt, Y. R. Chemla, S. B. Smith, C. Bustamante, *Annu. Rev. Biochem.*, 2008, **77**, 205–228.
31 M. Zhong, X. Wei, J. Zhou, Z. Wang, Y. Li, *Nat. commun.*, 2013, **4**, 1768.
32 P. Xia, J. Zhou, X. Song, B. Wu, X. Liu, D. Li, S. Zhang, Z. Wang, H. Yu, T. Ward, J. Zhang, Y. Li, X. Wang, Y. Chen, Z. Guo, X. Yao, *J. Mol. Cell Biol.*, 2014, **6**, 240-254.
33 S. W. Schmidt, M. K. Beyer, H. Clausen-Schaumann, *J. Am. Chem. Soc.*, 2008, **130**, 3664-3668.
34 B. Lin, J. Yu, S. A. Rice, *Phys. Rev. E*, 2000, **62**, 3909.
35 K. Visscher, S. P. Gross, S. M. Block, *IEEE J. Sel. Top. Quantum Electron.*, 1996, **2**, 1066-1076.
36 K. C. Vermeulen, G. J. Wuite, G. J. Stienen, C. F. Schmidt, *Appl. Opt.*, 2006, **45**, 1812-1819.
37 R.C. Gonzalez, R.E. Woods, S.L. Eddins, Digital image processing using MATLAB, Pearson Education India, Delhi, India, 2004.